

Bone morphogenetic protein 7 enhances the osteogenic differentiation of human dermal-derived CD105⁺ fibroblast cells through the Smad and MAPK pathways

FUGUO CHEN, DAN BI, CHEN CHENG, SUNXIANG MA, YANG LIU and KAIXIANG CHENG

Department of Plastic and Reconstructive Surgery, Shanghai Ninth People's Hospital,
Shanghai Jiao Tong University School of Medicine, Shanghai 200011, P.R. China

Received December 15, 2017; Accepted August 17, 2018

DOI: 10.3892/ijmm.2018.3938

Abstract. The skin, as the largest organ of the human body, is an important source of stromal stem cells with multipotent differentiation potential. CD105⁺ mesenchymal stem cells exhibit a higher level of stemness than CD105⁻ cells. In the present study, human dermal-derived CD105⁺ fibroblast cells (CD105⁺ hDDFCs) were isolated from human foreskin specimens using immunomagnetic isolation methods to examine the role of bone morphogenetic protein (BMP)-7 in osteogenic differentiation. Adenovirus-mediated recombinant BMP7 expression enhanced osteogenesis-associated gene expression, calcium deposition, and alkaline phosphatase activity. Investigation of the underlying mechanisms showed that BMP7 activated small mothers against decapentaplegic (Smad) and p38/mitogen-activated protein kinase signaling in CD105⁺ hDDFCs. The small interfering RNA-mediated knockdown of Smad4 or inhibition of p38 attenuated the BMP7-induced enhancement of osteogenic differentiation. In an *in vivo* ectopic bone formation model, the adenovirus-mediated overexpression of BMP7 enhanced bone formation from CD105⁺ hDDFCs. Taken together, these data indicated that adenoviral BMP7 gene transfer in CD105⁺ hDDFCs may be developed as an effective tool for bone tissue engineering.

Introduction

Fibroblasts, the main constituents of connective tissue, are a well-known source of cells for use in regenerative medicine owing to their ability to produce extracellular matrix

molecules and several bioactive factors (1,2). Human fibroblasts are cultured *in vitro* for investigative purposes and as a replacement therapy for damaged tissue, as they can be reprogrammed into a pluripotent state that can differentiate into different phenotypes (3,4). Human skin is an accessible source of multipotent stromal cells (MSCs) with self-renewal and multipotent capacities, which makes them valuable for various MSC-based therapies (5). MSCs can differentiate into adipocytes, osteocytes, and chondrocytes, and are characterized by the expression of three surface markers, CD105, CD90, and CD73 (6). Dermal fibroblasts with multipotent capacity express high levels of CD105, and CD73⁻ CD105⁺ fibroblasts have high proliferation rates and adipocyte/osteocyte differentiation potential (5,7).

Bone morphogenetic proteins (BMPs) are dimeric proteins that bind to type I and type II BMP receptors, transducing signals through small mothers against decapentaplegic (Smad)-dependent and -independent pathways to regulate the transcription of BMP target genes (8). BMP7 is a member of the transforming growth factor- β (TGF- β) superfamily, which possesses a high osteogenic capacity (9). BMPs signal via the p38 class of mitogen-activated protein kinases (MAPKs), and the activity of p38 MAPK is regulated by BMP signaling (10). The role of BMP7 in the osteogenic differentiation of human adipose-derived stem cells (ADSCs) has been investigated extensively (11). In addition, BMP4 and the BMP2/7 heterodimer have been shown to induce the osteogenic differentiation of mouse skin-derived fibroblasts (12). However, despite the potential therapeutic application of human dermal-derived fibroblasts (hDDFCs), the mechanisms underlying their osteogenic differentiation and the role of BMP7 in this process remain to be fully elucidated.

In the present study, human dermal-derived CD105⁺ fibroblast cells (CD105⁺ hDDFCs) were isolated to examine the role of BMP7 in the osteogenic differentiation of dermal fibroblast populations with multipotent stem cell capacity and investigate the underlying mechanisms.

Materials and methods

Immunomagnetic isolation of CD105⁺ hDDFCs and cell culture. The present study was performed in accordance

Correspondence to: Dr Fuguo Chen, Department of Plastic and Reconstructive Surgery, Shanghai Ninth People's Hospital, Shanghai Jiao Tong University School of Medicine, 639 Zhizaoju Road, Shanghai 200011, P.R. China
E-mail: chenfg5118@126.com

Key words: human dermal-derived CD105⁺ fibroblast cells, bone morphogenetic protein 7, osteogenic differentiation, p38 MAPK, Smad

with the Declaration of Helsinki for investigations involving human subjects, and was approved by the Ethics Committee of Shanghai Ninth People's Hospital Affiliated to Shanghai Second Medical University (Shanghai Ninth People's Hospital, Shanghai Jiao Tong University School of Medicine, Shanghai, China). Dermal fibroblasts were isolated from residual skin during circumcision surgery in 5 older children (age, 6-9 years) between June and July 2009. All patients provided written informed consent. The hDDFCs were isolated as described previously (13). Immunomagnetic isolation of the CD105⁺ cells was performed as described previously (14). Briefly, suspensions of hDDFCs obtained from human dermis were washed once with 1X PBS and resuspended with magnetic cell sorting (MACS) buffer (1X PBS containing 0.5% fetal bovine serum (FBS; cat. no. SH30087.01; HyClone; GE Healthcare Life Sciences, Logan, UT, USA) and 2 mM ethylenediamine tetraacetic acid, pH 7.2). A nylon mesh was used to filter cell suspensions (30- μ m pore). The cells were resuspended in MACS buffer at 10⁷ cells per 80 μ l, mixed with 20 μ l microbeads of directly conjugated mouse anti-human CD105 antibody (1:200; cat. no. MCA1557; Bio-Rad Laboratories, Inc., Hercules, CA, USA), and incubated at 4°C for 15 min on a rotator in the dark. Following washing in 1X PBS, the DDFCs-CD105 cells were resuspended in MACS buffer and processed in an LS⁺/VS⁺ separation column. The column was removed from the magnetic device, and the cells were flushed out with MACS buffer. The CD105⁻ and CD105⁺ cells were recovered by centrifugation at 300 x g for 10 min at 4°C for future use.

To determine the purity of the CD105⁺ cells, the cells were analyzed using the FACSCalibur device (BD Biosciences, San Jose, CA). Aliquots containing 0.5x10⁶ CD105⁺ cells were incubated with phycoerythrin (PE)-conjugated anti-CD105 antibody (1:100; cat. no. FAB10971B, R&D Systems, Inc., Minneapolis, MN, USA) on ice for 30 min, washed three times, and resuspended in wash buffer. IgG-PE (1:200; cat. no. SC-3756; Santa Cruz Biotechnology, Inc., Dallas, TX, USA) was used as the isotype control. The hDDFCs were suspended basal media, which consisted of DMEM (DMEM-HG; Invitrogen, Thermo Fisher Scientific, Inc., Waltham, MA, USA) supplemented with 10% FBS (HyClone; GE Healthcare Life Sciences) and maintained in the original culture medium at 37°C with 5% CO₂.

Construction of recombinant adenoviruses. The AdCMV-hBMP7 and AdCMV-LacZ viruses were generated by Shanghai Key Laboratory of Tissue Engineering (Shanghai, China) using the BD Adeno-X α expression system (BD Biosciences). *In vitro* ligation was used to incorporate a mammalian expression cassette into a replication-incompetent (Δ E1/ Δ E3) human adenoviral type 5 (Ad5) genome. Full-length human BMP7 (hBMP7) cDNA and pBlue-BMP7 (4.5 kb), obtained from the American Tissue Culture Collection (Manassas, VA, USA) were cloned into a shuttle vector via the *Kpn*I and *Not*I sites. The expression cassette was excised from the recombinant pShuttle2 plasmid using the *PI-Sce*I and *I-Ceu*I restriction endonucleases and ligated into the BD Adeno-X viral DNA. The recombinant linearized pAdeno-X DNA (*Pac*I digestion) was transfected into 293 cells (Type Culture Collection of the Chinese Academy of Sciences,

Shanghai, China) using FuGENE 6 (Roche Diagnostics, Basel, Switzerland) and the virus was purified by cesium chloride gradient ultracentrifugation at 100,000 x g for 2 h at 4°C and stored in 10% glycerol in PBS. Titers were determined by end-point dilution, yielding \sim 1.2x10¹⁰ plaque-forming units (pfu)/ml. Recombinant adenoviruses expressing β -galactosidase DNA (AdCMV-LacZ) were generated as controls.

Transduction of hDDFCs and treatment. The cultured CD105⁺ hDDFCs were harvested and treated with virus at a multiplicity of infection of 200 pfu/cell in 1 ml DMEM-HG medium for 4 h at 37°C. Following culture in DMEM with 10% FBS in a humidified atmosphere with 5% CO₂, the cells were harvested, counted, and resuspended in an alginate hydrogel at the indicated concentrations.

Small interfering RNAs (siRNAs) against Smad4 (target sequence: 5'-GCCATAGTGAAGGACTGTT-3') were synthesized by GeneChem (Shanghai, China). The hDDFCs (1x10⁵ cells) infected with recombinant adenovirus were transfected with Smad4 siRNA (2.5 μ g) for 48 h using Lipofectamine 2000 (Invitrogen, Thermo Fisher Scientific, Inc.). For inhibitor treatment, the recombinant adenovirus-infected CD105⁺ hDDFCs were incubated with osteogenic medium (OM) consisting of DMEM, 10% FBS, 1% antibiotics, 0.01 μ M 1,25-dihydroxyvitamin D3, 50 μ M ascorbate-2-phosphate, and 10 mM β -glycerophosphate (Sigma, EMD Millipore, Billerica, MA, USA) in the presence or absence of the p38 inhibitor (SB203580; 10 μ M; cat. no. tlr1-sb20; InvivoGen, San Diego, CA, USA) at 37°C for 24 h for western blot detection of p38 MAPK, 7 days for osteogenesis-associated gene expression, alkaline phosphatase (ALP) staining and ALP activity assay, and 21 days for Alizarin Red S staining.

Adipogenic differentiation. Adipogenic differentiation was performed as previously described (13). Briefly, the cells were cultured at 37°C on cover slips at a density of 3,000 cells/cm² in adipogenic differentiation medium consisting of low-glucose DMEM, 10% FBS, 1% antibiotics, 0.5 mM isobutylmethylxanthine, 1 μ M dexamethasone, 10 μ M insulin, and 200 μ M indomethacin (Sigma, EMD Millipore) for 3 weeks. To confirm differentiation, the cells were stained with Oil Red O (Sigma, EMD Millipore) for 5 min following induction, and photographed under an Axiovert inverted microscope (Zeiss AX10; Carl Zeiss AG, Oberkochen, Germany).

Osteogenic differentiation. Osteogenic differentiation was examined as previously described (13). Briefly, the cells were seeded at a density of 3,000 cells/cm² and cultured at 37°C in OM consisting of DMEM, 10% FBS, 1% antibiotics, 0.01 μ M 1,25-dihydroxyvitamin D3, 50 μ M ascorbate-2-phosphate, and 10 mM β -glycerophosphate. Alizarin Red S staining was performed 4 weeks following induction to confirm calcium deposition.

ALP staining was performed using the BCIP/NBT Alkaline Phosphatase Color Development kit (Beyotime Institute of Biotechnology, Jiangsu, China) following 7 days of osteogenic induction. ALP activity was assessed using an Alkaline Phosphatase Yellow (pNpp) Liquid Substrate system

for ELISA (Sigma, EMD Millipore) following 7 days of osteogenic induction.

Reverse transcription-quantitative polymerase chain reaction (RT-qPCR) analysis. Total RNA was extracted from the hDDFCs using TRIzol reagent (Invitrogen, Thermo Fisher Scientific, Inc.). For the synthesis of first strand cDNA, AMV reverse transcriptase (Promega, Madison, WI, USA) was used. qPCR was then performed using the SYBR Premix Ex Taq kit (Takara Biotechnology Co., Ltd., Dalian, China), in a volume of 25 μ l containing 2 μ l cDNA, 12.5 μ l SYBR Premix Ex Taq, 0.5 μ l each of the forward and reverse primers, and 9.5 μ l RNase-free water, in an ABI 7900 sequence detection system under the following conditions: Initial denaturation at 95°C for 10 min, followed by 40 cycles of denaturation at 95°C for 15 sec, annealing at 60°C for 30 sec, and extension at 72°C for 30 sec. The samples were then normalized to the expression of GAPDH using the $2^{-\Delta\Delta C_q}$ method (15). The following primers were used for qPCR: BMP7, sense 5'-GGG CTTCTCCTACCCCTACA-3' and antisense 5'-ACGTCT CATTGTCGAAGCGT-3'; osteopontin (OPN), sense 5'-AGG CCAAATAGAGCTGCCT-3' and antisense 5'-GTGGTC ATGGCTTTCGTTGG-3'; osteocalcin (OCN), sense 5'-CGT AGAAGCGCCGATAGGC-3' and antisense 5'-ATGAGA GCCCTCACACTCCTC-3'; osterix (OSX), sense 5'-CTC TGCGGGACTCAACAAC-3' and antisense 5'-ATGGAT GCCTGCCTTGACC-3'; runt related transcription factor 2 (RUNX2), sense 5'-TCTGGCCTTCCACTCTCAGT-3' and antisense 5'-GTCCACTCTGGCTTGGGAA-3'; ALP, sense 5'-ACCGCTTCCCATATGTGGCT-3' and antisense 5'-GGT CTGGAAGTTGCCCTTGA-3'; GAPDH, sense 5'-ACCATC TTCCAGGAGCGAGA-3' and antisense 5'-TGTTTACA CCCATGACGAA-3'.

Western blot analysis. Protein was extracted from the cells using RIPA buffer and protein concentration was quantified with a BCA kit (Bio-Rad Laboratories, Inc., Richmond, CA, USA). Aliquots of cell lysates containing equal quantities of protein (30 μ g) were separated by 12% SDS-PAGE and transferred onto nitrocellulose membranes (Amersham, GE Healthcare Life Sciences, Chalfont, UK). The membranes were blocked with 5% nonfat milk in TBST overnight, and incubated with primary antibodies against p-Smad 1/5/8 (1:1,000; cat. no. 9511), Smad1 (1:1,000; cat. no. 9743), extracellular signal-regulated kinase (ERK; 1:2,000; cat. no. 4696), phosphorylated (p)-ERK (1:1,000; cat. no. 9101), c-Jun N-terminal kinase (JNK; 1:1,000; cat. no. 9252), and p-JNK (1:1,000; cat. no. 9251) from Cell Signaling Technology, Inc. (Beverly, MA, USA); p-p38 (1:500; cat. no. sc-7973), p38 (1:1,000; cat. no. sc-7972), BMP7 (1:200; cat. no. sc-9305), runt-related transcription factor 2 (RUNX2; 1:1,000; cat. no. sc-12488), and ALP (1:200; cat. no. sc-15065) from Santa Cruz Biotechnology, Inc.; and OSX (1:500; cat. no. ab94744), OPN (1:1,000; cat. no. ab8448), OCN (1:500; cat. no. ab93876) and GAPDH (1:2,000; cat. no. ab22555) from Abcam (Cambridge, UK) at 4°C overnight. The membranes were then washed three times in TBST, and incubated with the corresponding horseradish peroxidase-conjugated secondary antibodies (1:5,000; cat. no. 31462 and 32230; both from Thermo Fisher Scientific, Inc.) at 4°C for 1 h. Signals were detected using the Pierce

ECL western blotting substrate. The quantification of western blot bands was conducted by comparison against the GAPDH bands using ImageJ software (version 1.48; National Institutes of Health, Bethesda, MD, USA).

Induction of bone formation by hBMP7-transduced fibroblasts in vivo. A total of 10 immunodeficient C57BL/6 male mice aged 4-5 weeks (15 ± 0.30 g) were obtained from Shanghai Second Medical University Center of Laboratory Animals (Shanghai, China). All experimental protocols were approved by the Animal Experiment Committee of Shanghai Second Medical University. Mice had *ad libitum* access to food and water and were maintained in a 12-h light/dark cycle at $21\pm 2^\circ\text{C}$ with a relative humidity of $45\pm 10\%$. The mice were injected with CD105⁺ hDDFCs transfected with Ad-LacZ (negative control) or Ad-BMP7. Alginate (Sigma, EMD Millipore) was dissolved in PBS to a concentration of 2% (w/v), and the adenovirus-infected CD105⁺ hDDFCs were added to the alginate solution at a density of 2.5×10^7 cells/ml. The cell-alginate preparation was mixed with excessive aqueous slurries of 2M calcium chloride to produce hydrogels and washed with PBS. The mice were anesthetized and injected subcutaneously with two 400 μ l injections of cell-hydrogel mixture using an 18-gauge needle into the dorsal panniculus carnosus. The Ad-BMP7-transduced cells were injected into the right side and Ad-LacZ-transduced cells were injected into the left side of mice. At 12 weeks post-implantation, the mice were sacrificed by CO₂ asphyxiation. Bone constructs were dissected and surrounding soft tissue was removed. X-ray images were acquired and the bone constructs were fixed in 4% paraformaldehyde for the histologic and immunohistochemical analyses of bone formation.

Bone formation was monitored *in vivo* by fixing bone constructs with 4% paraformaldehyde, followed by decalcification in 10% formic acid. The samples were dehydrated in a graded alcohol series, diaphonized in xylene, and embedded in paraffin. The paraffin blocks were sectioned into 5- μ m-thick slides, deparaffinized, hydrated, stained with hematoxylin and eosin (H&E) and photographed under an Axiovert inverted microscope (Zeiss AX10).

Statistical analysis. The results are expressed as the mean \pm standard deviation. Student's t-test was used for comparisons of two groups and one-way analysis of variance was used for multiple comparisons. Data were analyzed using SPSS software (version 14.0; SPSS, Inc., Chicago, IL, USA). $P<0.05$ was considered to indicate a statistically significant difference.

Results

Isolation and in vitro differentiation of CD105⁺ cells from hDDFCs. Primary CD105⁺ hDDFCs exhibited an extended and long narrow shape, whereas CD105⁺ hDDFCs exhibited a spindle-like morphology following 12 h in culture (Fig. 1A). Flow cytometric analysis confirmed the expression of the surface marker CD105 in isolated cells and the isolated CD105⁺ cells had a purity of $95\pm 2.5\%$ (Fig. 1B). The differentiation of hDDFCs into osteogenic and adipogenic lineages was confirmed by Alizarin red staining and Oil-red-O staining

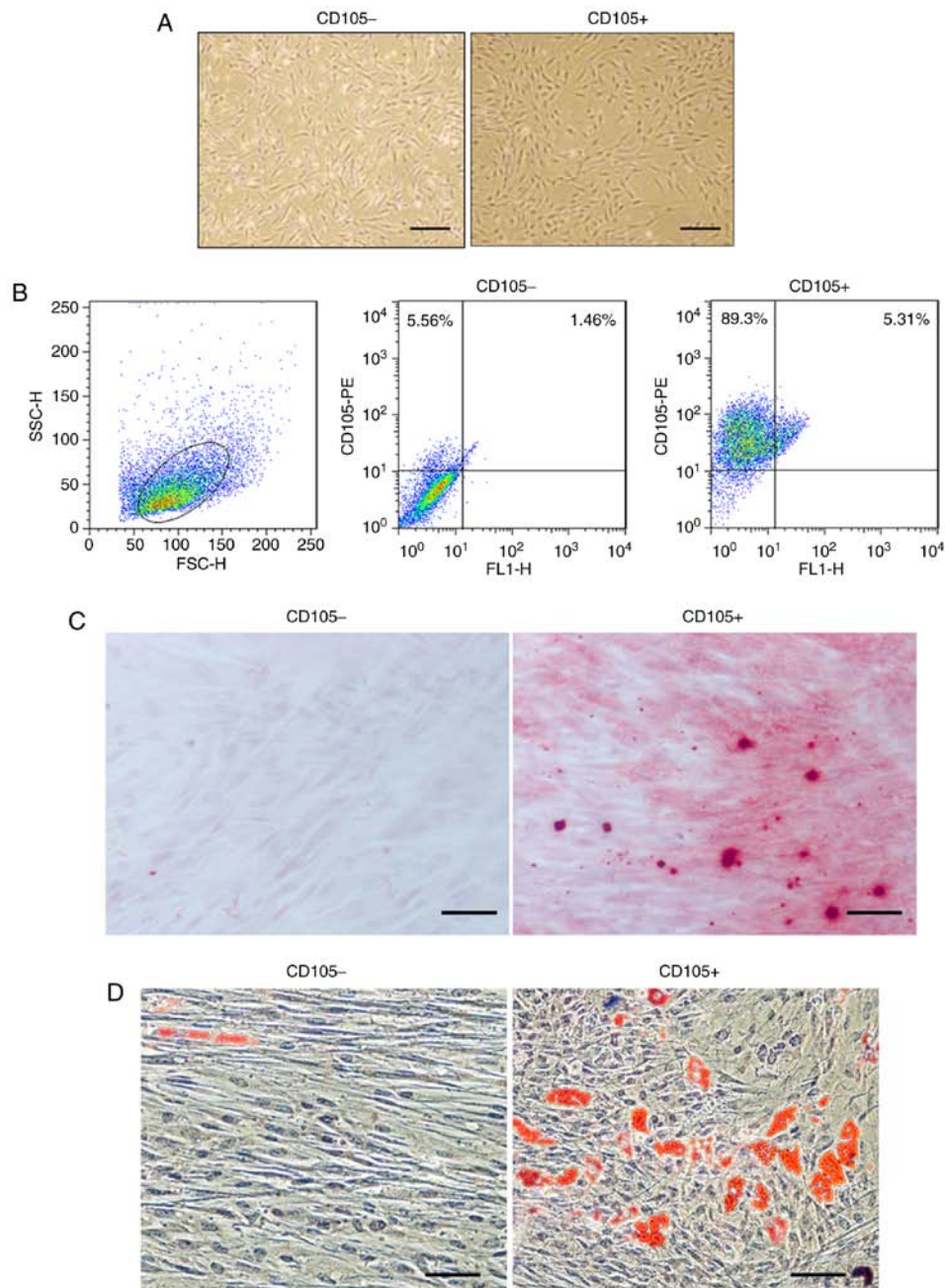


Figure 1. Morphological and flow cytometry analyses of human dermis-derived CD105⁺ fibroblastic cells (CD105⁺ hDDFCs). (A) Morphology of CD105⁻ and CD105⁺ hDDFCs obtained following 12 h of culture. Scale bar=200 μm. (B) Cell purity following magnetic sorting was assessed by FACS analysis. Debris were excluded on the FSC/SSC plot. Multiple differentiation potential of CD105⁻ and CD105⁺ hDDFCs was examined via (C) Alizarin Red staining analysis of the differentiation of CD105⁺ hDDFCs to an osteogenic lineage; (D) Oil red O staining analysis of differentiation into an adipogenic lineage. Scale bar=100 μm. hDDFCs, human dermal-derived fibroblast cells.

3-4 weeks following induction. Representative images of Alizarin red- and Oil-red-O-stained CD105⁻ and CD105⁺ cells are shown in Fig. 1C and D.

BMP7 enhances the osteogenic differentiation of CD105⁺ hDDFCs. To examine the effect of BMP7 on the osteogenic differentiation potential of CD105⁺ hDDFCs, the cells were infected with recombinant adenovirus expressing hBMP7 and cultured in BM or OM. The expression of BMP7 and osteogenesis-associated genes was assessed by RT-qPCR and western blot analyses. The results showed that the expression levels of RUNX2, OSX, OCN, OPN, and ALP were

significantly upregulated by OM, and BMP7 significantly enhanced this effect (Fig. 2A and B). Alizarin red staining at 21 days post-osteogenic induction showed that BMP7 enhanced the intensity of staining, indicating increased calcium deposition (Fig. 2C). BMP7 significantly increased the expression and activity of ALP by ~1.5-fold in the cells cultured in OM (Fig. 2D and E). Taken together, these results indicated that BMP7 has a potent effect on enhancing the osteogenic differentiation of CD105⁺ hDDFCs.

Activation of Smad and MAPK signaling in CD105⁺ hDDFCs. The present study further examined the mechanisms underlying

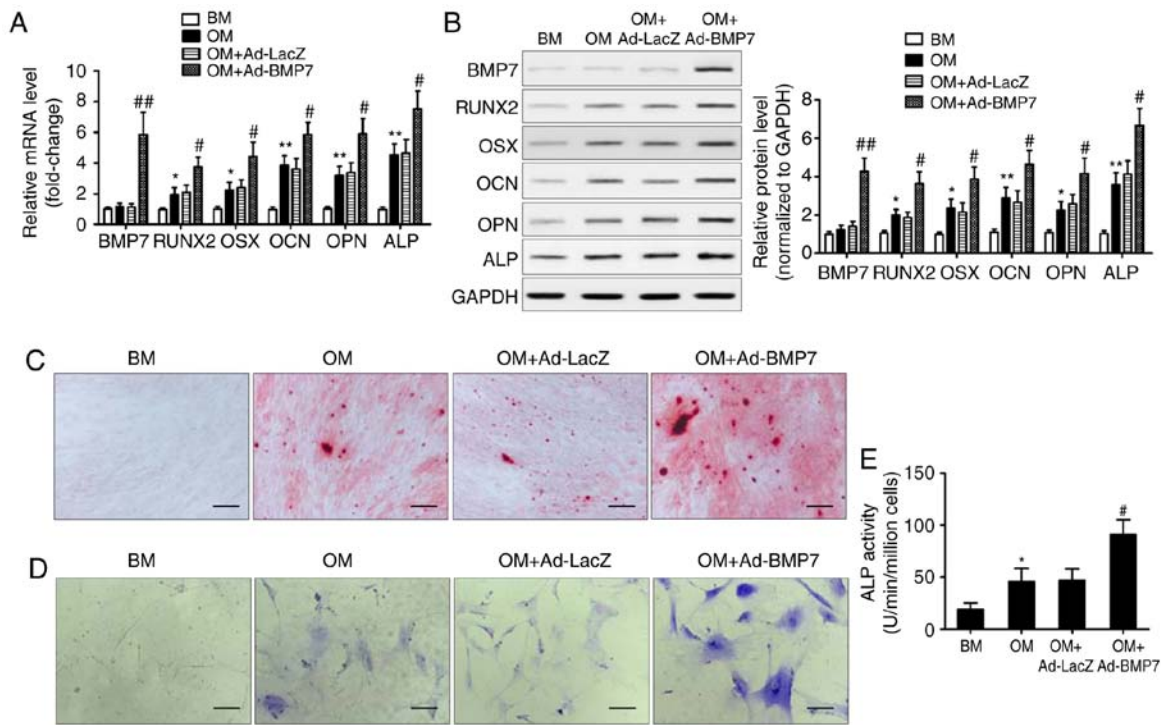


Figure 2. BMP7 promotes the osteogenic differentiation of CD105⁺ hDDFCs *in vitro*. CD105⁺ hDDFCs were infected with recombinant adenovirus expressing human BMP7 for 48 h and cultured in BM or OM. Detection of BMP7 and osteogenesis-associated gene expression by (A) reverse transcription-quantitative polymerase chain reaction and (B) western blot analyses at 7 days. Densitometric quantification of the immunoblot normalized to GAPDH. *P<0.05 and **P<0.01, vs. BM; #P<0.05 and ##P<0.01, vs. OM+Ad-LacZ. Osteogenic differentiation of CD105⁺ hDDFCs infected with or without recombinant adenovirus in the presence of BM or OM was determined by (C) Alizarin Red S at 21 days, (D) ALP staining at 7 days, and an (E) ALP activity assay at 7 days. Scale bar=200 μm. *P<0.05, vs. BM; #P<0.05, vs. OM+Ad-LacZ. hDDFCs, human dermal-derived fibroblast cells; BM, basal medium; OM, osteogenic medium; BMP7, bone morphogenetic protein 7; RUNX2, runt related transcription factor 2; OSX, osterix; OCN, osteocalcin; OPN, osteopontin; ALP, alkaline phosphatase.

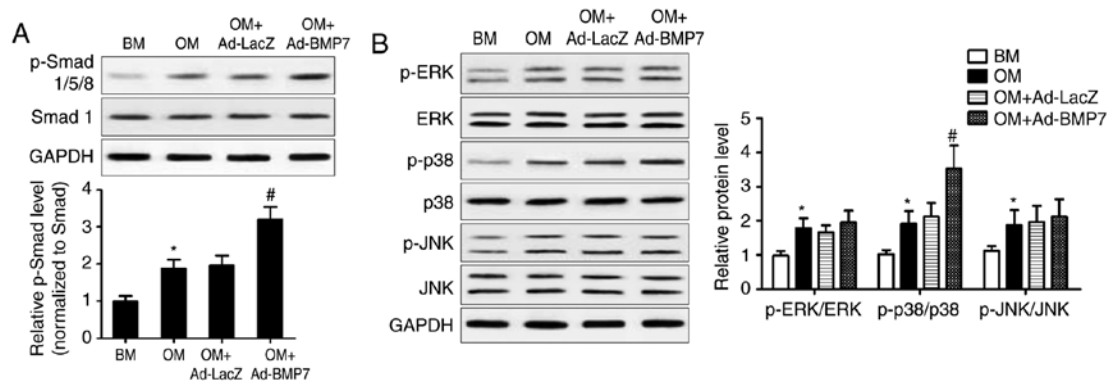


Figure 3. BMP7 activates Smad and MAPK pathways in CD105⁺ hDDFCs cells. CD105⁺ hDDFCs or BMP7-expressing adenovirus-infected CD105⁺ hDDFCs were treated with BM or OM, and the phosphorylation of (A) Smad- and (B) MAPK-related proteins was analyzed by western blot analysis following 24 h of culture. Densitometric quantification of the immunoblot normalized to total protein. *P<0.05, vs. BM; #P<0.05, vs. OM+Ad-LacZ. hDDFCs, human dermal-derived fibroblast cells; BMP7, bone morphogenetic protein 7; BM, basal medium; OM, osteogenic medium; Smad, small mothers against decapentaplegic; MAPK, mitogen-activated protein kinase; ERK, extracellular signal-regulated kinase; JNK, c-Jun N-terminal kinase; p-, phosphorylated.

the effect of BMP7 on the osteogenic differentiation of CD105⁺ hDDFCs by assessing the expression of proteins associated with the BMP canonical Smad-dependent and non-canonical Smad-independent pathways. The results of the western blot analysis and densitometric quantification showed that BMP7-expressing adenovirus infection significantly enhanced the OM-induced upregulation of p-Smad1/5/8, indicating the activation of Smad signaling (Fig. 3A). OM treatment induced the phosphorylation of ERK, p38 and JNK, and the overexpression of BMP7 further upregulated the OM-induced

phosphorylated form of p38 (Fig. 3B). These results indicated the activation of p38/MAPK signaling by BMP7 in the CD105⁺ hDDFCs.

Smad4 knockdown impairs the promotion of osteogenic differentiation of CD105⁺ hDDFCs induced by BMP7. To further elucidate the involvement of the Smad pathway in the effect of BMP7, the present study examined the effect of Smad4 knockdown on the enhancing effect of BMP7 on the OM-induced osteogenic differentiation of CD105⁺ hDDFCs.

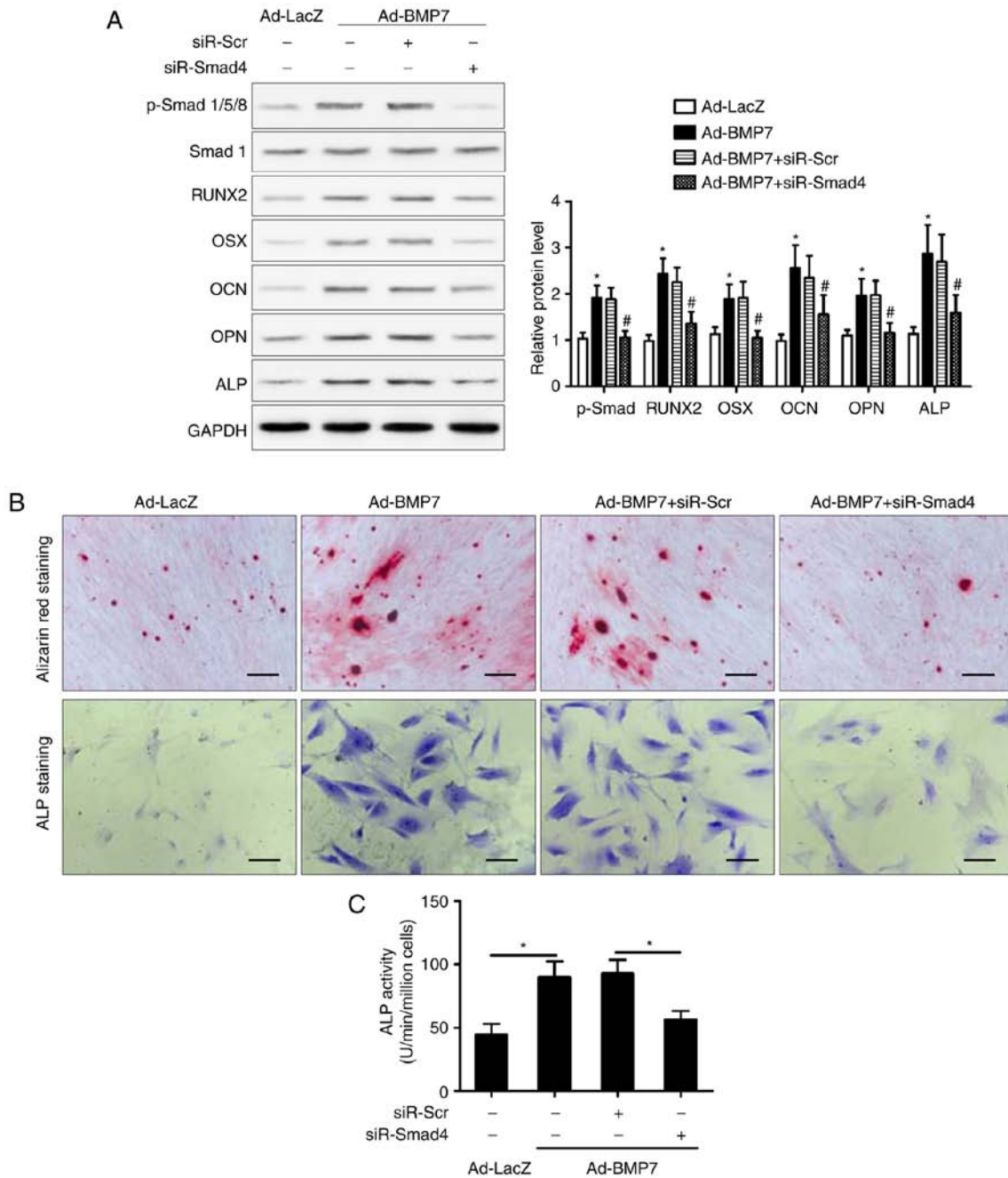


Figure 4. SMAD4 knockdown attenuates the BMP7-induced promotion of CD105⁺ hDDFCs osteogenic differentiation. (A) Recombinant adenovirus-infected CD105⁺ hDDFCs transfected with siRNA for Smad4 or control were subjected to western blot analysis for the detection of Smad/p-Smad and osteogenesis-associated gene expression 7 days following osteogenic induction. Densitometric quantification of p-Smad was normalized to total Smad; densitometric quantification of other proteins was normalized to GAPDH. * $P < 0.05$, vs. Ad-LacZ; # $P < 0.05$, vs. Ad-BMP7+siR-Scr. Osteogenic differentiation of CD105⁺ hDDFCs infected with or without recombinant adenovirus in presence of osteogenic medium was determined by (B) Alizarin Red S and ALP staining and an (C) ALP activity assay 7 or 21 days following osteogenic induction. Scale bar=200 μm . * $P < 0.05$. hDDFCs, human dermal-derived fibroblast cells; Smad, small mothers against decapentaplegic; siR, small interfering RNA; Scr, scramble; BMP7, bone morphogenetic protein 7; RUNX2, runt related transcription factor 2; OSX, osterix; OCN, osteocalcin; OPN, osteopontin; ALP, alkaline phosphatase; p-, phosphorylated.

The silencing of Smad eliminated the BMP7-induced upregulation of RUNX2, OSX, OCN, OPN and ALP in the presence of OM, compared with that in the si-Control transfected cells (Fig. 4A). Consistent with these results, Smad knockdown reversed the BMP7-induced increase in Alizarin red and ALP staining (Fig. 4B) and ALP activity (Fig. 4C), indicating that the effect of BMP7 on promoting the osteogenic differentiation of CD105⁺ hDDFCs occurred via a Smad-dependent pathway. The expression of p38 MAPK (p38/p-p38) was also measured

and the results showed that it was not altered by siR-Smad4 (data not shown).

Inhibition of p38/MAPK attenuates the osteogenic differentiation of CD105⁺ hDDFCs induced by BMP7. To determine the role of the p38 MAPK pathway, the cells were treated with the p38 inhibitor SB203580 and incubated in OM in the presence or absence of BMP7. The results of the western blot analysis showed that inhibition of p38 attenuated the

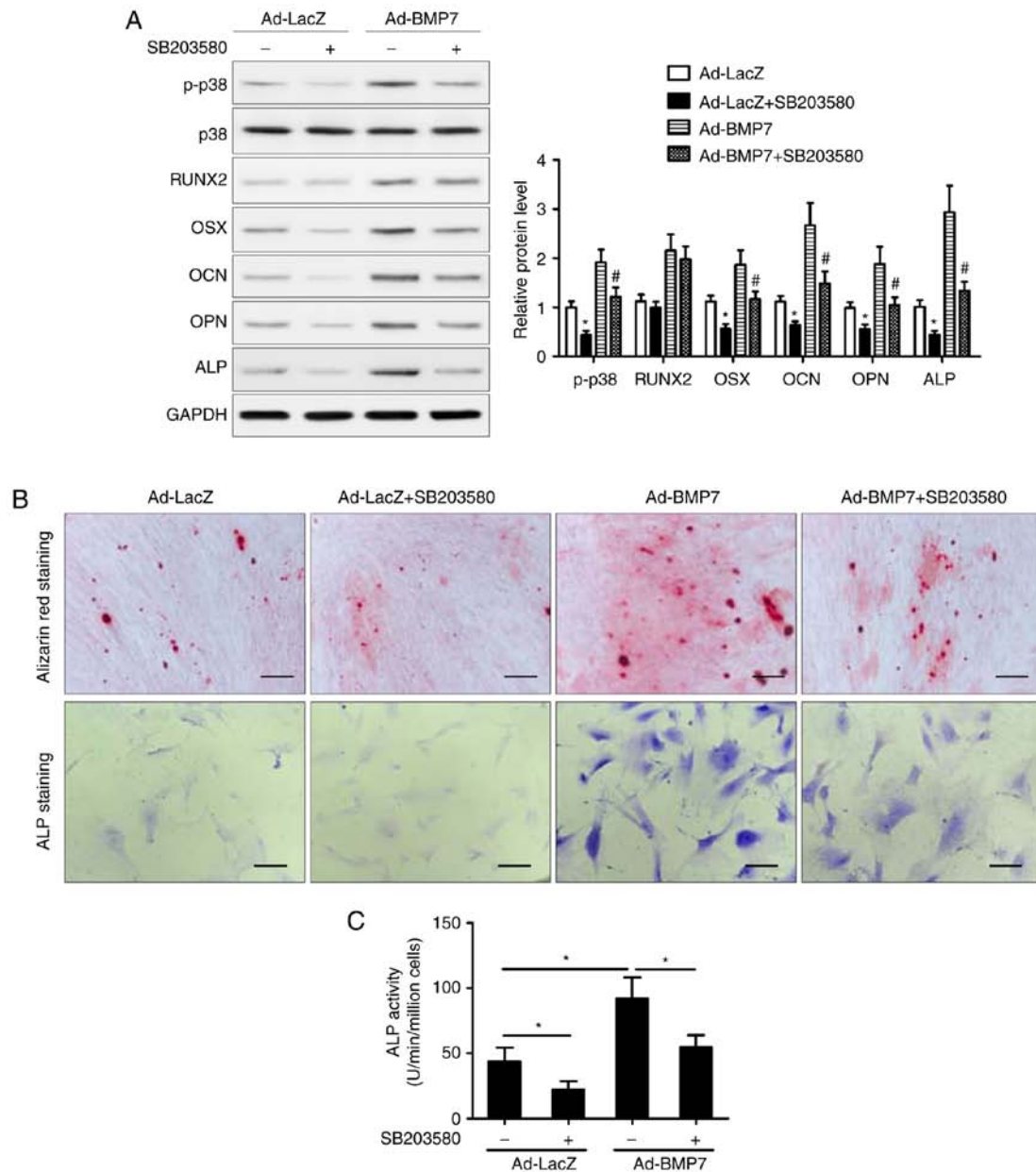


Figure 5. Inhibition of p38 MAPK attenuates the BMP7-induced promotion of CD105⁺ hDDFCs osteogenic differentiation. Recombinant adenovirus infected CD105⁺ hDDFCs were incubated with OM in the presence or absence of the p38 inhibitor (SB203580, 10 μ M). (A) Western blot detection of p38 MAPK following 24 h of culture in OM, and osteogenesis-associated gene expression 7 days following osteogenic induction. Densitometric quantification of p-p38 was normalized to total p38; densitometric quantification of other proteins was normalized to GAPDH. *P<0.05, vs. Ad-LacZ; #P<0.05, vs. Ad-BMP7. Osteogenic differentiation of CD105⁺ hDDFCs infected with or without recombinant adenovirus in the presence of BM or OM was determined by (B) Alizarin Red S and ALP staining, and an (C) ALP activity assay 7 or 21 days following osteogenic induction. Scale bar=200 μ m. *P<0.05. hDDFCs, human dermal-derived fibroblast cells; BMP7, bone morphogenetic protein 7; BM, basal medium; OM, osteogenic medium; Smad, small mothers against decapentaplegic; BMP7, bone morphogenetic protein 7; RUNX2, runt related transcription factor 2; OSX, osterix; OCN, osteocalcin; OPN, osteopontin; ALP, alkaline phosphatase; p-, phosphorylated.

BMP7-induced upregulation of OSX, OCN, OPN, and ALP, whereas the expression of RUNX2 was not affected by the inhibition of p38 (Fig. 5A). The Alizarin red and ALP staining showed that the inhibition of p38 attenuated the effect of BMP7 on enhancing the OM-induced osteogenic differentiation of CD105⁺ hDDFCs (Fig. 5B). In addition, treatment with SB203580 reversed the BMP7-induced increase in ALP activity (Fig. 5C). Taken together, these results indicated that the p38 MAPK signaling pathway was involved in the enhancement of the OM-induced osteogenic differentiation of CD105⁺ hDDFCs by BMP7. The results also showed that p38

inhibitor SB203580 suppressed BMP7-induced Smad1/5/8 phosphorylation (data not shown).

BMP7 enhances bone formation of CD105⁺ hDDFCs in vivo. The effects of BMP7 on osteogenic differentiation were examined in nude mice injected intramuscularly with adenovirus infected CD105⁺ hDDFCs. Representative X-ray images and bone volumes from mice are shown in Fig. 6A, indicating enhanced bone formation by BMP7 *in vivo*. The H&E staining of tissue sections showed enhanced trabecular bone formation in Ad-BMP7 sections compared with Ad-LacZ sections

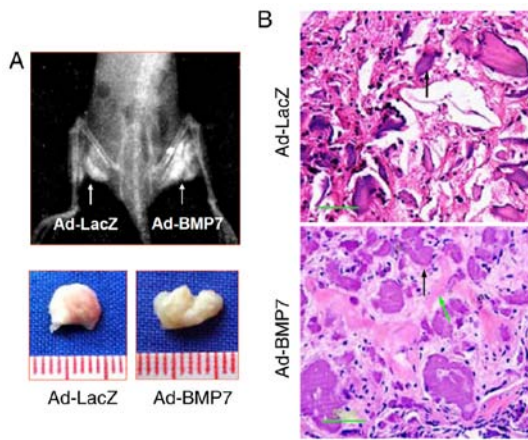


Figure 6. BMP7 induces bone formation of CD105⁺ hDDFCs cells *in vivo*. Adenovirus-infected CD105⁺ hDDFCs with calcium alginate were injected intramuscularly into nude mice (n=5). (A) X-ray images of opaque tissue were captured and bone volumes were measured at 12 weeks post-injection. (B) Hematoxylin and eosin staining of tissue sections. Scale bar=50 μ m. Green arrows indicate trabecular bone generated by osteocyte-like cells; black arrows indicate undegraded alginate material. hDDFCs, human dermal-derived fibroblast cells; BMP7, bone morphogenetic protein 7.

(Fig. 6B). These results confirmed the effect of BMP7 on promoting the osteogenic differentiation of CD105⁺ hDDFCs in an *in vivo* model.

Discussion

The adult mammalian dermis contains a subpopulation of precursor cells that possess the capacity to differentiate into different lineages (16-18). These fibroblastic MSCs have attracted attention for their plasticity and, therefore, their potential therapeutic applications, including in transplantation for bone formation (19). In the present study, the role of BMP7 in the osteogenic differentiation of CD105⁺ hDDFCs was examined *in vitro* and *in vivo*, and the underlying Smad-dependent and -independent mechanisms were identified.

Conflicting reports exist on the differentiation potential of dermal fibroblasts, with certain studies suggesting limited potential and others demonstrating adipocytic, osteocytic and chondrocytic differentiation capacities (20-23). One reason for these controversial results is the heterogeneity of isolated dermal fibroblasts, which include populations with different differentiation capacities (5,13). Although dermal fibroblasts have a surface antigen profile similar to that of MSCs and ADSCs, human foreskin-derived dermal fibroblasts do not always have the potential to differentiate into adipogenic or osteogenic lineages. This is a result of only a fraction of dermal-derived fibroblasts being positive for CD105, and the expression of CD105 determines the properties of MSCs (5,24). In the present study, a CD105⁺ subpopulation of hDDFCs was isolated from human foreskin specimens and it was shown that they possessed the capacity to differentiate into osteogenic and adipogenic lineages by incubation in the corresponding induction medium. Furthermore, the overexpression of BMP7 via adenovirus infection enhanced the BM-induced osteogenic differentiation of CD105⁺ hDDFCs. In a previous study, rat dermal fibroblasts transduced with an adenovirus vector engineered to express BMP7 were transplanted into

immunocompromised mice. These transduced dermal fibroblasts formed bone and repaired skeletal defects, indicating the role of BMP7 in promoting bone formation *in vivo* (25). Similarly, BMP7-transduced dermal fibroblasts repaired segmental defects in rat femurs when injected subcutaneously, and only BMP7-transduced fibroblasts formed bone in diffusion chambers, suggesting that BMP induces osteoblastic differentiation of fibroblasts (22). These studies support the findings of present study and suggest that further investigations is warranted to assess the potential of BMP7-expressing CD105⁺ hDDFCs for *in vivo* applications.

To investigate the mechanisms underlying the effect of BMP7 on the osteogenic differentiation of CD105⁺ hDDFCs, the present study examined Smad-dependent and -independent pathways. The results showed that the overexpression of BMP7 enhanced the OM-induced activation of Smad and MAPK signaling. Furthermore, Smad4 knockdown or the inhibition of p38 MAPK signaling suppressed the effect of BMP7 on enhancing the OM-induced osteogenic differentiation of CD105⁺ hDDFCs, indicating the involvement of the two signaling pathways. The role of the BMP/Smad pathways in regulating osteoblast differentiation has been investigated extensively (26). TGF- β signals are transmitted through the formation of type I and type II serine/threonine kinase receptor complexes (27). The conserved canonical TGF- β /BMP signaling cascade depends on cell surface BMP receptors that mediate the phosphorylation of Smad proteins, which translocate into the nucleus to regulate the transcription of specific genes (28). In the non-canonical Smad-independent signaling pathway, the activation of p38 MAPK mediates the differentiation of mesenchymal precursor cells (29). In response to BMP induction, the Smad and p38 MAPK pathways converge at the Runx2 gene to control MSC differentiation, and the activity of Runx2 and BMP-activated Smads is essential for bone formation. The results of the present study showed that the expression of Runx2 was not affected by p38 MAPK inhibition; further experiments are required to determine the involvement of Runx2 in the BMP7-induced osteogenic differentiation of CD105⁺ hDDFCs. However, the present study demonstrated the involvement of the two pathways in the effect of BMP7. BMP2-induced osteogenic differentiation and increased bone formation have previously been shown to be mediated by the activation of Smad and p38 signaling pathways in MC3T3-E1 preosteoblasts (30). Crosstalk between these two pathways and other signaling pathways, including Wnt, Hedgehog and Notch, are key in BMP signaling; therefore, understanding the mechanisms underlying their effect on the induction of osteoblastogenesis and bone formation is essential for their clinical application (31-35).

In the present study, an *in vivo* ectopic bone formation model was used to confirm that the ectopic expression of BMP7 enhanced bone formation in nude mice injected intramuscularly with adenovirus-infected CD105⁺ hDDFCs. The increasing use of BMP-containing osteogenic implants for the treatment of bone-related diseases requires the development of effective delivery systems and cell sources. The present study provides a rationale for the use of skin-derived precursors with the potential to differentiate into an osteogenic lineage and demonstrated their efficacy *in vivo*. This provides the basis for further investigations to establish systems for the use of subpopulations of hDDFCs as a cellular source for tissue engineering.

In conclusion, the present study showed that a subpopulation of dermal fibroblasts with positive expression of CD105 offer potential for osteogenic differentiation, which is enhanced by the induction of BMP7 and mediated by the activation of Smad and p38/MAPK signaling. These data indicate that adenoviral BMP7 gene transfer in CD105⁺ hDDFCs may be an effective tool for bone tissue engineering.

Acknowledgements

Not applicable.

Funding

This study was supported by the National Natural Science Foundation of China (grant no. 81272126).

Availability of data and materials

All data used and/or analysed during the present study are available from the corresponding author on reasonable request.

Authors' contributions

FC made substantial contributions to the design of this study and wrote the manuscript. DB and CC performed experiments. SM, YL and KC performed data analysis. DB, CC, SM, YL and KC revised the critically. All authors read and approved the final manuscript and agreed to the publication of the final manuscript.

Ethics approval and consent to participate

The present study was performed in accordance with the Declaration of Helsinki for investigations involving human subjects, and was approved by the Ethics Committee of Shanghai Ninth People's Hospital Affiliated to Shanghai Second Medical University (Shanghai Ninth People's Hospital, Shanghai Jiao Tong University School of Medicine). All patients provided written informed consent. All animal experiment protocols were approved by the Animal Experiment Committee of Shanghai Second Medical University.

Patient consent for publication

Not applicable.

Competing interests

The authors declare that they have no competing interests.

References

- Sorrell JM and Caplan AI: Fibroblasts—a diverse population at the center of it all. *Int Rev Cell Mol Biol* 276: 161-214, 2009.
- Fang F, Ni K, Cai Y, Ye Z, Shang J, Shen S and Xiong C: Biological characters of human dermal fibroblasts derived from foreskin of male infertile patients. *Tissue Cell* 49: 56-63, 2017.
- Bussmann BM, Reiche S, Marí-Buyé N, Castells-Sala C, Meisel HJ and Semino CE: Chondrogenic potential of human dermal fibroblasts in a contractile, soft, self-assembling, peptide hydrogel. *J Tissue Eng Regen Med* 10: E54-E62, 2016.
- Guerreiro SG, Oliveira MJ, Barbosa MA, Soares R and Granja PL: Neonatal human dermal fibroblasts immobilized in RGD-alginate induce angiogenesis. *Cell Transplant* 23: 945-957, 2014.
- Lee SB, Shim S, Kim MJ, Shin HY, Jang WS, Lee SJ, Jin YW, Lee SS and Park S: Identification of a distinct subpopulation of fibroblasts from murine dermis: CD73(-) CD105(+) as potential marker of dermal fibroblasts subset with multipotency. *Cell Biol Int* 40: 1008-1016, 2016.
- Dominici M, Le Blanc K, Mueller I, Slaper-Cortenbach I, Marini F, Krause D, Deans R, Keating A, Prockop DJ and Horwitz E: Minimal criteria for defining multipotent mesenchymal stromal cells. The International Society for cellular therapy position statement. *Cytotherapy* 8: 315-317, 2006.
- Lorenz K, Sicker M, Schmelzer E, Ruff T, Salvetter J, Schulz-Siegmund M and Bader A: Multilineage differentiation potential of human dermal skin-derived fibroblasts. *Exp Dermatol* 17: 925-932, 2008.
- Miyazono K, Maeda S and Imamura T: BMP receptor signaling: Transcriptional targets, regulation of signals, and signaling cross-talk. *Cytokine Growth Factor Rev* 16: 251-263, 2005.
- Chen G, Deng C and Li YP: TGF- β and BMP signaling in osteoblast differentiation and bone formation. *Int J Biol Sci* 8: 272-288, 2012.
- Lee KS, Hong SH and Bae SC: Both the Smad and p38 MAPK pathways play a crucial role in Runx2 expression following induction by transforming growth factor-beta and bone morphogenetic protein. *Oncogene* 21: 7156-7163, 2002.
- Zhang X, Guo J, Wu G and Zhou Y: Effects of heterodimeric bone morphogenetic protein-2/7 on osteogenesis of human adipose-derived stem cells. *Cell Prolif* 48: 650-660, 2015.
- Myllylä RM, Haapasaari KM, Lehenkari P and Tuukkanen J: Bone morphogenetic proteins 4 and 2/7 induce osteogenic differentiation of mouse skin derived fibroblast and dermal papilla cells. *Cell Tissue Res* 355: 463-470, 2014.
- Chen FG, Zhang WJ, Bi D, Liu W, Wei X, Chen FF, Zhu L, Cui L and Cao Y: Clonal analysis of nestin(-) vimentin(+) multipotent fibroblasts isolated from human dermis. *J Cell Sci* 120: 2875-2883, 2007.
- Aslan H, Zilberman Y, Kandel L, Liebergall M, Oskouian RJ, Gazit D and Gazit Z: Osteogenic differentiation of noncultured immunoisolated bone marrow-derived CD105⁺ cells. *Stem Cells* 24: 1728-1737, 2006.
- Livak KJ and Schmittgen TD: Analysis of relative gene expression data using real-time quantitative PCR and the 2(-Delta Delta C(T)) method. *Methods* 25: 402-408, 2001.
- Crigler L, Kazhanie A, Yoon TJ, Zakhari J, Anders J, Taylor B and Virador VM: Isolation of a mesenchymal cell population from murine dermis that contains progenitors of multiple cell lineages. *FASEB J* 21: 2050-2063, 2007.
- Toma JG, Akhavan M, Fernandes KJ, Barnabé-Heider F, Sadikot A, Kaplan DR and Miller FD: Isolation of multipotent adult stem cells from the dermis of mammalian skin. *Nat Cell Biol* 3: 778-784, 2001.
- French MM, Rose S, Canseco J and Athanasiou KA: Chondrogenic differentiation of adult dermal fibroblasts. *Ann Biomed Eng* 32: 50-56, 2004.
- Hirata K, Tsukazaki T, Kadowaki A, Furukawa K, Shibata Y, Moriishi T, Okubo Y, Bessho K, Komori T, Mizuno A and Yamaguchi A: Transplantation of skin fibroblasts expressing BMP-2 promotes bone repair more effectively than those expressing Runx2. *Bone* 32: 502-512, 2003.
- Brendel C, Kuklick L, Hartmann O, Kim TD, Boudriot U, Schwel D and Neubauer A: Distinct gene expression profile of human mesenchymal stem cells in comparison to skin fibroblasts employing cDNA microarray analysis of 9600 genes. *Gene Expr* 12: 245-257, 2005.
- Jeney F, Bazsó-Dombi E, Oravecz K, Szabó J and Nagy IZ: Cytochemical studies on the fibroblast-preadipocyte relationships in cultured fibroblast cell lines. *Acta Histochem* 102: 381-389, 2000.
- Rutherford RB, Moalli M, Franceschi RT, Wang D, Gu K and Krebsbach PH: Bone morphogenetic protein-transduced human fibroblasts convert to osteoblasts and form bone in vivo. *Tissue Eng* 8: 441-452, 2002.
- Mizuno S and Glowacki J: Low oxygen tension enhances chondroinduction by demineralized bone matrix in human dermal fibroblasts in vitro. *Cells Tissues Organs* 180: 151-158, 2005.
- Lysy PA, Smets F, Sibille C, Najimi M and Sokal EM: Human skin fibroblasts: From mesodermal to hepatocyte-like differentiation. *Hepatology* 46: 1574-1585, 2007.

25. Krebsbach PH, Gu K, Franceschi RT and Rutherford RB: Gene therapy-directed osteogenesis: BMP-7-transduced human fibroblasts form bone in vivo. *Hum Gene Ther* 11: 1201-1210, 2000.
26. Mao CY, Wang YG, Zhang X, Zheng XY, Tang TT and Lu EY: Double-edged-sword effect of IL-1beta on the osteogenesis of periodontal ligament stem cells via crosstalk between the NF-kappaB, MAPK and BMP/Smad signaling pathways. *Cell Death Dis* 7: e2296, 2016.
27. Moustakas A, Souchelnytskyi S and Heldin CH: Smad regulation in TGF-beta signal transduction. *J Cell Sci* 114: 4359-4369, 2001.
28. Guo X and Wang XF: Signaling cross-talk between TGF-beta/BMP and other pathways. *Cell Res* 19: 71-88, 2009.
29. Beederman M, Lamplot JD, Nan G, Wang J, Liu X, Yin L, Li R, Shui W, Zhang H, Kim SH, *et al*: BMP signaling in mesenchymal stem cell differentiation and bone formation. *J Biomed Sci Eng* 6: 32-52, 2013.
30. Choi H, Jeong BC, Kook MS and Koh JT: Betulinic acid synergistically enhances BMP2-induced bone formation via stimulating Smad 1/5/8 and p38 pathways. *J Biomed Sci* 23: 45, 2016.
31. Horikiri Y, Shimo T, Kurio N, Okui T, Matsumoto K, Iwamoto M and Sasaki A: Sonic hedgehog regulates osteoblast function by focal adhesion kinase signaling in the process of fracture healing. *PLoS One* 8: e76785, 2013.
32. Reichert JC, Schmalzl J, Prager P, Gilbert F, Quent VM, Steinert AF, Rudert M and Nöth U: Synergistic effect of Indian hedgehog and bone morphogenetic protein-2 gene transfer to increase the osteogenic potential of human mesenchymal stem cells. *Stem Cell Res Ther* 4: 105, 2013.
33. Kim JH, Liu X, Wang J, Chen X, Zhang H, Kim SH, Cui J, Li R, Zhang W, Kong Y, *et al*: Wnt signaling in bone formation and its therapeutic potential for bone diseases. *Ther Adv Musculoskelet Dis* 5: 13-31, 2013.
34. Bessa PC, Casal M and Reis RL: Bone morphogenetic proteins in tissue engineering: The road from the laboratory to the clinic, part I (basic concepts). *J Tissue Eng Regen Med* 2: 1-13, 2008.
35. Rahman MS, Akhtar N, Jamil HM, Banik RS and Asaduzzaman SM: TGF- β /BMP signaling and other molecular events: Regulation of osteoblastogenesis and bone formation. *Bone Res* 3: 15005, 2015.



This work is licensed under a Creative Commons Attribution-NonCommercial-NoDerivatives 4.0 International (CC BY-NC-ND 4.0) License.